
 ◎ Technical Paper

A Comparison of Proposed Wave Model with Various Wave Models

Sun Hong Kwon* and Dong Dai Ha**

(Received April 22, 1988)

제시한 해양파 모델과 다른 모델들과의 비교

권 순 홍 · 하 동 대

Key Words: Ocean Wave Model(해양파모델), Wave Spectrum(파 스펙트럼), Wave Model Intercomparison(해양파모델 상호비교)

초 록

해양에서 바람에 의해 생성된 파도를 예측하는 모델을 제시하고 이 모델에 대한 개략적인 설명과 아울러 분류에 의한 기존 모델들을 소개하고 마지막으로 이 모델을 유한폭의 해양에 대하여 적용한 결과를 기존의 다른 모델들과 비교하였다.

1. Introduction

In recent years a significant amount of researches has been made on the development of numerical wave models. A lot of wave forecasting models are in operation now around the world. Since most wave models perform with varying degrees of accuracy, the wave model intercomparison study to clarify the interrelations among the various wave models has been very active. The first principal results of the intercomparison study of deep water wave models are presented jointly by the Sea Wave Modeling Project (SWAMP) Group¹⁾. The Shallow Water Intercomparison of Wave Model (SWIM) Project²⁾ is a follow up project of the SWAMP.

In this study a proposed numerical wave model is compared with the various models. The proposed wave model, VPINK, was developed by Neu and

Kwon³⁻⁵⁾. VPINK is a decoupled propagation (DP) wave model. Those models used in the intercomparison have been developed in the past years for the real time wave forecasting and regional wave statistics compilation. Table I lists the various models used in intercomparison study. VENICE is a decoupled propagation (DP) model, as is the case with VPINK. SAIL and BMO are

Table 1 Models used in intercomparison

Country	Model name	Model class	Applications
USA	SAIL	CD	Regional wave statistics
UK	BMO	CD	Operational forecast Atlantic
Norway	NOWAMO	CH	Operational forecast Northeast Atlantic
Holland	GONO	CH	Operational forecast Atlantic
Italy	VENICE	DP	Regional wave statistics

+ 1988년도 한국해양공학회 춘계 학술대회 발표(1988년 6월)

* Member, Dept. of Naval Architecture, Pusan National University

** Dept. of Naval Architecture, Pusan National University

classified as a coupled discrete (CD) model. NO-WAMO and GONO are the coupled hybrid (CH) model. Since VPINK itself is the decoupled propagation wave model, only one extra DP model is adopted.

First, fetch and duration limited growth test case is considered. The growth of the spectra as a function of fetch and time is presented. The first generation models exhibit nested spectral growth. The next is the 90° change in wind direction test case. The purpose of this test is to study the relaxation process in which windsea results in a relaxation of the wave field toward a new sea state. The computational results of these models presented in the Sea Wave Modeling Project (SWAMP) Group are quoted.

2. Model Classes

The rate of change of the wave spectrum can be described by energy balance equation (Hasselmann⁹)

$$\frac{\partial E}{\partial t} + \vec{C}_g \cdot \Delta E = S = S_{in} + S_{nl} + S_{ds} \quad (2.1)$$

where E is the wave spectrum, \vec{C}_g is the group velocity of this spectral component and Δ is the horizontal gradient operator. The term on the left hand side of equation(2.1) governs the propagation of the wave spectrum. S represents the sum of individual source functions. S_{in} , S_{nl} , and S_{ds} represent the wind input, nonlinear wave-wave interaction, and dissipation source functions respectively. Most of numerical models in the present operations computes the wave spectrum by integrating the equation. The major differences are the source functions. The understanding of those terms is the ultimate object of muth current research on wave prediction. S_{in} has been the subject of intense interest for a long time. Starting with the pioneering theories of Phillips⁶) and Miles⁷⁻¹⁰) The energy input from the wind S was represented as

$$S_{in} = A + BE \quad (2.2)$$

The A term represents energy transfer from the turbulent pressure fluctuations to the wave field

according to the theory of Phillips. The BE term represents the interaction of an already disturbed surface with the wind due to the Miles. S_{ds} is the least well known both theoretically and experimentally. This term became effective when the spectrum reached a saturation limit. Of the three terms, S_{nl} is at present best known, having been derived theoretically by Hasselmann¹¹).

In the first generation decoupled propagation models(DP), the wave growth is dominated by wind energy input and the spectrum is discretized into frequency and direction bands. Each band is allowed to evolve more or less independently and propagates at its own group velocity in its own direction. Barnett¹²) and Ewing¹³) included the nonlinear transfer explicitly but they represented the nonlinear transfer with small modification. Their wave growth and spectral forms are dominated by the wind input. Thus they class these models as first generation models. Other models of this type include those of Gelci and Chavy¹⁴) and Pierson¹⁵). The second generation wave models implicitly employ nonlinear transfer as the dominant mechanism controlling the spectral shape. These attempt to parameterize the nonlinear transfer instead of trying to calculate the three dimensional nonlinear Boltzmann integral expression for nonlinear source function (Hasselmann,¹¹) which are too much time consuming to evaluate.

The coupled hybrid models represented the evolution of swell as a decoupled discrete spectral model since the nonlinear coupling between the swell and windsea can be neglected. Models of this type include those of Hasselmann, et al.¹⁶) and Gunther, et al.¹⁷). But this coupled hybrid model(CH) may find difficulties in treating the windsea-swell transition regime in which the nonlinear energy redistribution is neither negligible nor dominant. This can be treated by adopting the traditional discrete spectral representation for the windsea and swell regions. We refer those models as coupled discrete (CD) models. These include the models of Resio¹⁸) and Golding¹⁹).

3. Structure of the Model

VPINK is a decoupled propagation wave model, suitable for finite ocean applications. Only a short description of VPINK will be given here. Readers interested in the details of the model are referred to the paper quoted.

VPINK starts from the version of the energy balance equation (Hasselmann, ¹¹)

$$\begin{aligned} \frac{E(f, \theta; \vec{x}, t)}{\partial t} + \vec{C}_g \cdot \Delta E(f, \theta; \vec{x}, t) &= S(f, \theta; \vec{x}, t) \\ &= S_{in} + S_{nl} + S_{ds} \end{aligned} \quad (3.1)$$

where E is the two dimensional directional frequency wave spectrum being a function of position \vec{x} , time t , wave frequency f , and direction of propagation θ . \vec{C}_g is the group velocity of the spectral component and S represents the sum of individual source functions. S_{in} , S_{nl} , and S_{ds} represent the wind input, nonlinear wave interaction and dissipation source functions respectively. The nonlinear wave-wave interaction is neglected in this theory.

The energy input from the wind S_{in} is represented as

$$S_{in} = A(u, f, \alpha) + B(u^*, f, \alpha) E(f, \theta, \vec{x}, t) \quad (3.2)$$

where u is the wind velocity, u^* is the friction velocity and α is the angle between wind and wave directions. The $A(u, f, \alpha)$ term is based on the theory of Phillips. ⁶) Phillips mechanism represents the generation of waves on an initially calm water surface through the turbulent atmospheric pressure fluctuations. A form of the A term is adopted

$$\begin{aligned} A(f, u_{6,1}, \alpha) &= A_1(f, u_{6,1}, \alpha) \text{ if } \frac{w}{u_{6,1}} \leq 0.02 \\ A(f, u_{6,1}, \alpha) &= A_2(f, u_{6,1}, \alpha) \text{ if } \frac{w}{u_{6,1}} > 0.02 \end{aligned} \quad (3.3)$$

where

$$\begin{aligned} A_1(f, u_{6,1}, \alpha) &= \frac{4.73 \times 10^{-16} w^4 u_{6,1}^3}{Q_1(w, u_{6,1}, \alpha) R_1(w, u_{6,1}, \alpha)} \\ A_2(f, u_{6,1}, \alpha) &= \frac{7.167 \times 10^{-14} w^{5.25} u_{6,1}^{1.75}}{Q_2(w, u_{6,1}, \alpha) R_2(w, u_{6,1}, \alpha)} \end{aligned} \quad (3.4)$$

and

$$\begin{aligned} Q_1 &= 0.2704 \left(\frac{w}{u_{6,1}} \right)^2 + \left(\frac{w^2}{g} \sin \theta \right)^2 \\ Q_2 &= Q_1 \end{aligned}$$

$$R_1 = 4.87 \times 10^{-6} + \left(\frac{w^2}{g} \cos \theta - \frac{w}{u_{6,1}} \right)^2$$

$$R_2 = 0.1089 \left(\frac{w^2}{g} \right)^{2.5} + \left(\frac{w^2}{g} \cos \theta - \frac{w}{u_{6,1}} \right)^2$$

A_1 and A_2 are in m^2/rad , $u_{6,1}$ wind velocity at 6.1 m above the water surface is in m/s . g is in m/s^2 .

The $B(u^*, f, \alpha) E(f, \theta; \vec{x}, t)$ term is the result of the interaction of the air flow with the already disturbed water surface. Miles ⁷⁻¹⁰) considered the perturbation of the mean shear flow in the air by the disturbed water surface, but he neglected the effects of atmospheric turbulence. Phillips ²⁰) extended the analysis to consider the interaction of the wave induced air flow perturbations with the free stream turbulence. The proposed final form of the B term is given

$$\begin{aligned} \frac{B}{f} &= \frac{\rho_a}{\rho_w C^2 K} \left\{ \frac{M_m N^2 K^4}{\cos^2 \alpha} \left(\frac{-U''}{(U')^3} \right)_{z_m} \left(\int_{z_m}^{\infty} [U(z) \cos \alpha - c] e^{-kz} dz \right)^2 \right. \\ &\quad \left. + M \int_0^{\infty} N^2 (-U'') \cos \alpha |U \cos - c| e^{-2kz} dz \right\} \end{aligned} \quad (3.5)$$

where the mean wind profile can be written as

$$U(z) = \frac{u^*}{\kappa} \ln \left(\frac{z}{z_0} \right) \quad (3.6)$$

κ is Von Karman's constant and z_0 is the roughness height. In this study Wu's expression ²¹) is adopted as

$$z_0 = 0.112 \frac{(u^*)^2}{g} \quad (3.7)$$

z_m is the matched layer height where the mean wind velocity matches the phase velocity of the wave. z_0 can be related with z_m as

$$z_0 = z_m \exp \left\{ \frac{-\kappa c}{u^* \cos \alpha} \right\} \quad (3.8)$$

$M_m = \pi$, $M = 1.6 \times 10^{-2}$, $N^2 = \frac{1}{3}$ for $z > z_m$, $N^2 = 1$ for $z < z_m$

VPINK model prevents the wave spectrum from growing above an assumed fully developed limit by balancing the input from the wind with the dissipation without explicitly modeling the dissipation for waves travelling with the wind. Due to the structure of the model, a limiting directional wave spectrum must be assumed as a function of wind speed. The form used here is the Pierson-Moskowitz ²²) spectrum with spreading function, which was derived by SWOP project (Cote, et al.) ²³)

The fully developed spectrum is thus

$$E_{\infty}(w, \alpha, u) = E_{\infty}(w, u) F(w, \alpha, u) \quad (3.9)$$

$$\text{where } E_{\infty}(w, u) = \gamma g^2 w^{-5} e^{-\left[\beta \left(\frac{w_0}{w}\right)^4\right]} \quad (3.10)$$

where $w = 2\pi f$, $w_0 = \frac{g}{u}$, u being the mean wind speed measured at 19.5 m above the sea surface, $\gamma = 8.1 \times 10^{-3}$ and $\beta = 0.074$

For a finite ocean, a modified Lax-Wendroff scheme due to Gadd²⁴⁻²⁶) is used to propagate the wave energy in two dimensions. For onedimensional propagation at speed c , the finite difference expression is represented as

$$E_{j+\frac{1}{2}}^{n+\frac{1}{2}} = \frac{1}{2} (E_j^n + E_{j+1}^n) - \frac{\mu}{2} (E_{j+1}^n - E_j^n) \quad (3.11)$$

$$E_j^{n+1} = E_j^n - \mu \left\{ (1+q)(E_{j+\frac{1}{2}}^{n+\frac{1}{2}} - E_{j-\frac{1}{2}}^{n+\frac{1}{2}}) \right.$$

$$\left. - \frac{q}{3} (E_{j+\frac{1}{2}}^{n+\frac{1}{2}} - E_{j-\frac{1}{2}}^{n+\frac{1}{2}}) \right\}$$

where $\sigma = \frac{C\Delta t}{\Delta x}$, $q = \frac{3}{4}(1-\sigma^2)$

j signifies spatial position and n the time level. For points one grid length from a boundary, q is set to zero. Along the boundary, upstream differences are used for outflow components while inflow values are specified. VPINK model uses 27 frequency bands, each of with 0.01 Hz, from 0.04 to 0.30 Hz and 18 directional bands each 20° wide, except where noted.

4. Numerical Applications and Results

The first case is the fetch and duration-limited growth case. The geometry of the wind field and boundary conditions are shown in Fig. 1. A stationary, homogeneous wind field with wind speed $U = 20 \text{ m/s}$ blows orthogonally offshore. The wind field is infinite in the lateral and downstream directions. The initial wave energy at time $t=0$ is zero, and the spectrum at coastline $y=0$ remains zero for $t>0$. The models were run until a stationary state was reached for the entire area. The purpose of the test was to investigate the relations between fetch and duration-limited wave growth for different models. The fully developed spectra of the compared models are shown in Fig.2. The

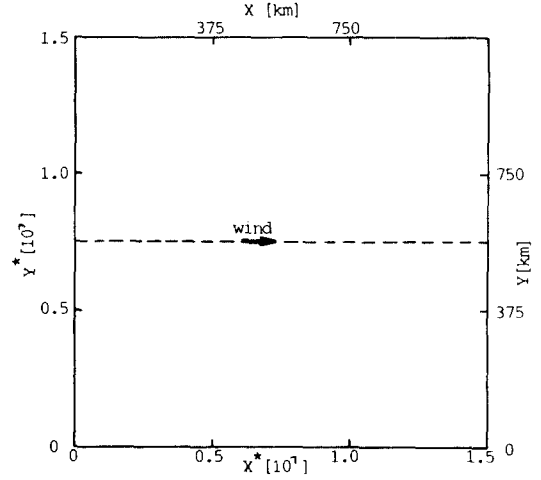


Fig. 1 Wind field geometry for fetch- and duration-limited growth

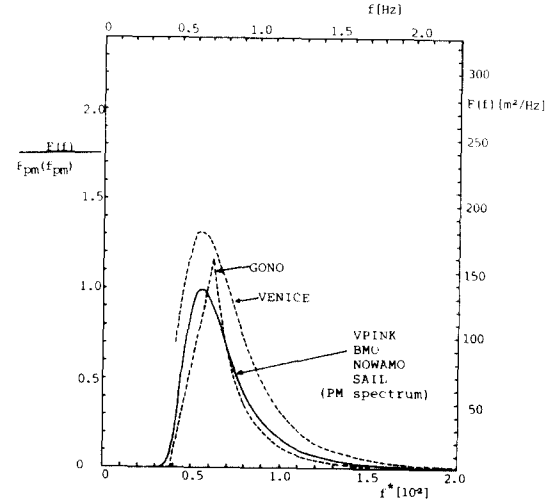


Fig. 2 Fully developed spectrum of the compared model

growth of the spectra as a function of fetch is shown in Fig.3. First generation decoupled propagation models exhibit nested spectral growth and are unable to reproduce the overshoot phenomenon, which is clearly seen in the second generation model SAIL. This is exemplified by VENICE and VPINK. The maximum spectrum of the VPINK could not make to reach 1. This is partly attributed to the fact that the discretized frequency could not exactly hit the Pierson-Moskowitz peak freq-

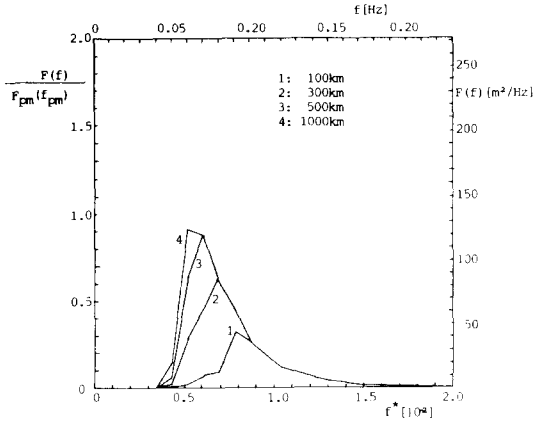


Fig. 3a Growth of the VPINK as a function of fetch

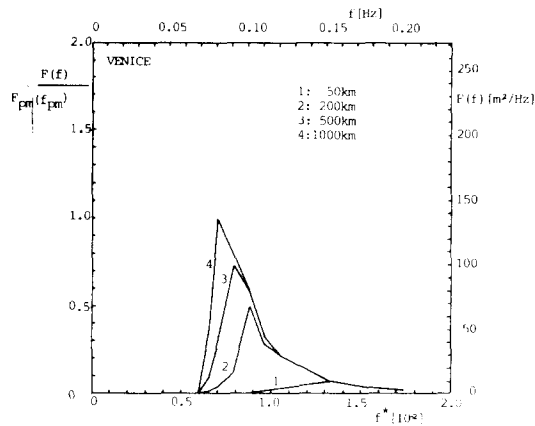


Fig. 3b Growth of the VENICE as a function of fetch

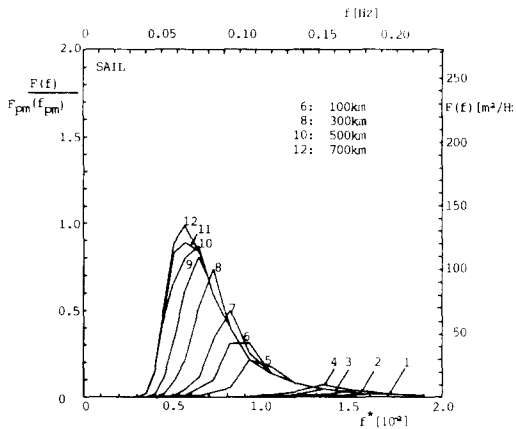


Fig. 3c Growth of the SAIL as a function of fetch

Another reason is that too much computational time made it very difficult to carry out the computation until sea reaches stationary state. Fig. 4 shows the nondimensional energy E , for all models as a function of x for large t (stationary state). The corresponding duration-limited growth curves for infinite fetch (in practice, $x=1000\text{ km}$) are shown in Fig. 5. The strong differences are apparent between different models in Figures 4 and 5. Much of this scatter might be caused by

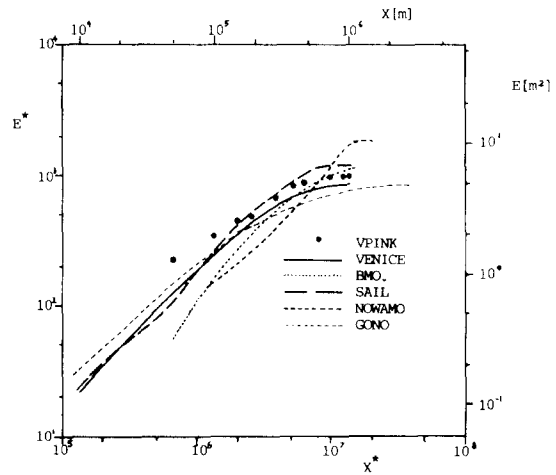


Fig. 4 Nondimensional fetch-limited growth curves for the total energy E^*

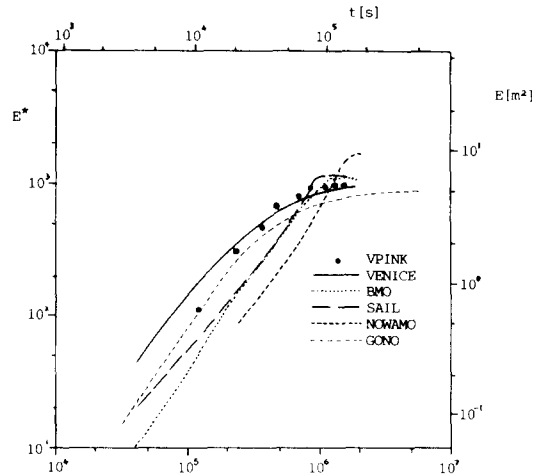


Fig. 5 Nondimensional duration-limited growth curves for the total energy E^*

the indeterminacy of the drag law relating u^* to u_{10} . The nondimensional fetchlimited and duration-limited growth curves of the VPINK for the total energy E show the relatively high growth. Note that the DP model VENICE also shows the relatively high growth.

The next is the 90° change in wind direction test case. A uniform wind blows to the north at 20 m/s over an infinite ocean until the sea is half-developed ($f_p = 2f_{pM}$). At this time ($t=0$) the wind is instantly turned 90° , from north to west, at the same wind speed, 20 m/s . If we consider an infinite ocean with homogenous wind, the wave spectrum is not a function of position. The numerical model for this case requires only one spacial grid point and no propagation scheme. At the instant the wind direction turns, the pre-existing windsea largely becomes swell and a new wind sea begins to grow. The purpose of the test is to study this relaxation process in which windsea results in a relaxation of the wind field toward a new steady sea state. There are three mechanisms which are believed to contribute to the relaxation. These are the energy input by the wind, attenuation of the swell, and nonlinear interactions, which transfer energy from the swell to the wind sea.

The results of this test case are presented in Figures 6.1~6.6. Angles are measured clockwise

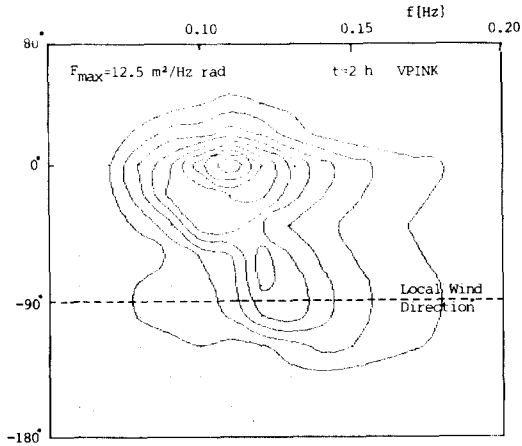


Fig. 6.1a Contour plot of the 2d spectral distribution for the DP model VPINK(contours are drawn at increment of 10% of the maximum spectral value present in each plot)

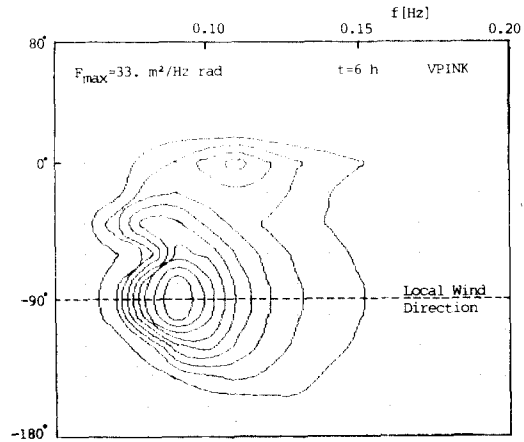


Fig. 6.1 b Same as Fig. 6.1 a for the DP model

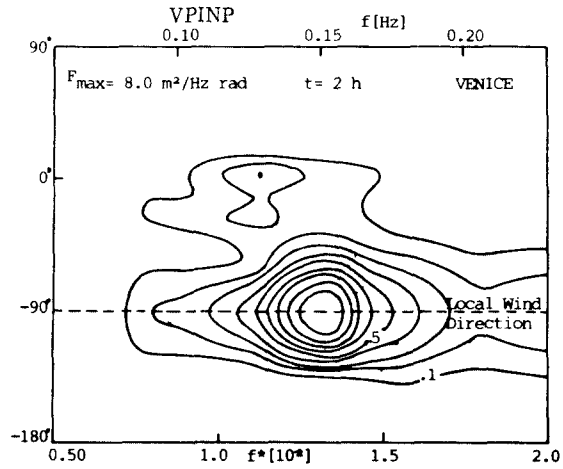


Fig. 6.2 a Same as Fig. 6.1 a for the DP model

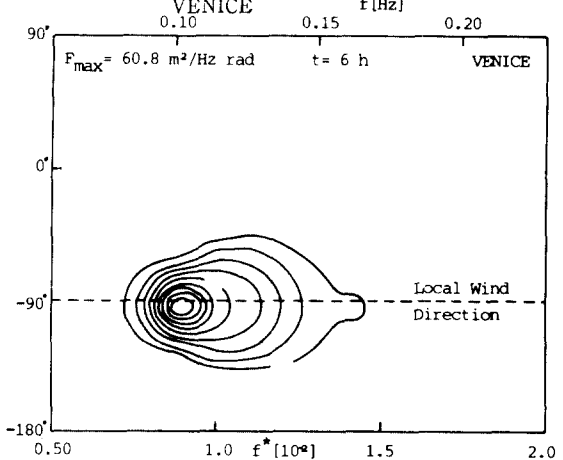


Fig. 6.2 b Same as Fig. 6.1 a for the DP model

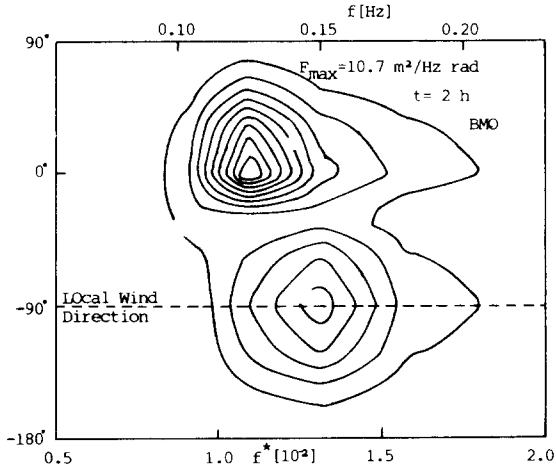


Fig. 6.3 a Same as Fig. 6.1 a for the CD model BMO

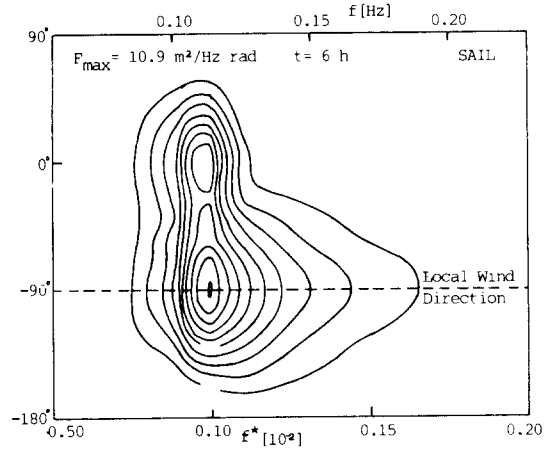


Fig. 6.4 b Same as Fig. 6.1 a for the CD model SAIL.

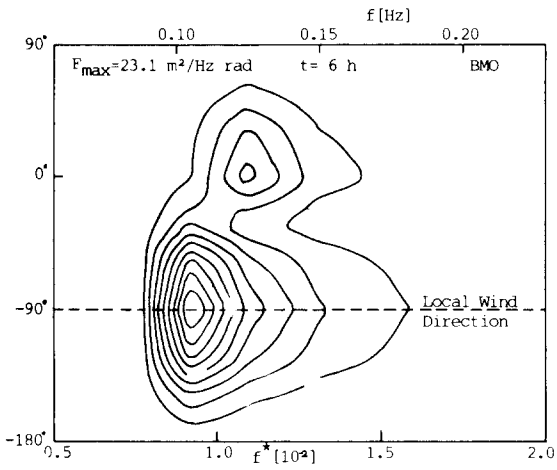


Fig. 6.3 b Same as Fig. 6.1 a for the CD model BMO

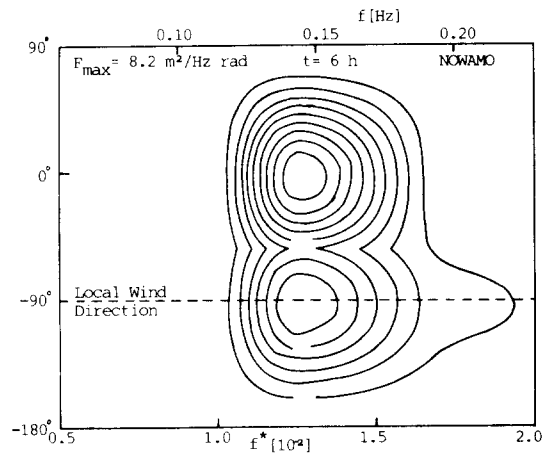


Fig. 6.5 Same as Fig. 6.1 a for the CH model NOWAMO

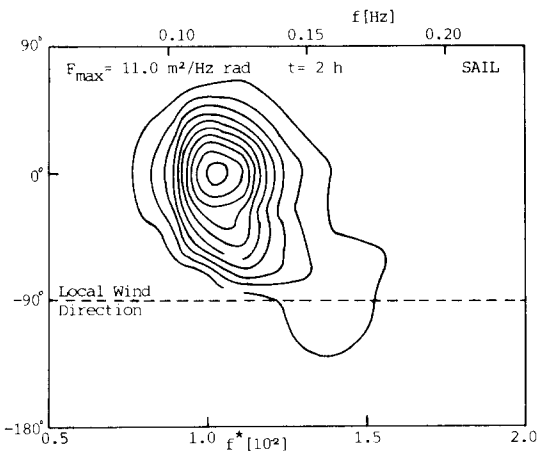


Fig. 6.4 a Same as Fig. 6.1 a for the CD model SAIL

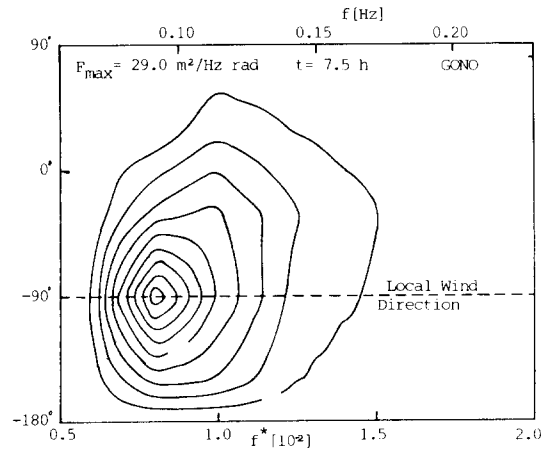


Fig. 6.6 Same as Fig. 6.1 a for the CH model GONO

from north. The spectra represented are two-dimensional spectra. The spectra are shown at 2 and 6 hours after the wind direction has changed when the spectra were half-developed. NOWAMO and GONO models show only at 6 and 7.5 hours, respectively. Since VPINK and VENICE are the decoupled propagation models, the nonlinear wave-wave interactions can not be described. Those models simply attenuate the swell field and generate a new superimposed windsea. The VENICE model shows relatively high swell energy dissipation rate in which the swell has completely decayed after 6 hours (Fig. 6.2 b). The curves from CD models and CH models reveal that no general parameterization of the nonlinear coupling between windsea and swell exists. The relative growth of the windsea and decay of the swell are seen in the growth curves of Fig. 7.1~7.6. The growth curves of the new windsea for the DP models show

relatively high growth which was already seen in duration-limited growth case. Most of the coupled models show negligible swell decay.

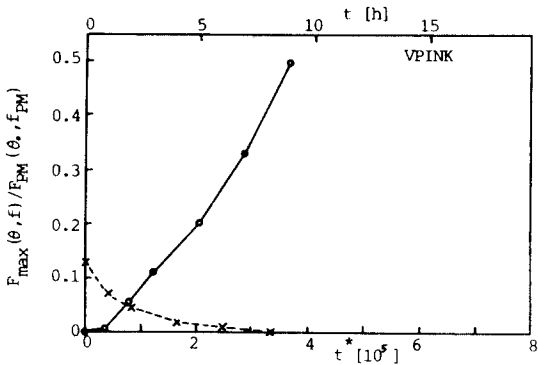


Fig. 7.1 Evolutions of the windsea(solid line) and swell(dashed line) peak spectral densities for the DP model VPINK

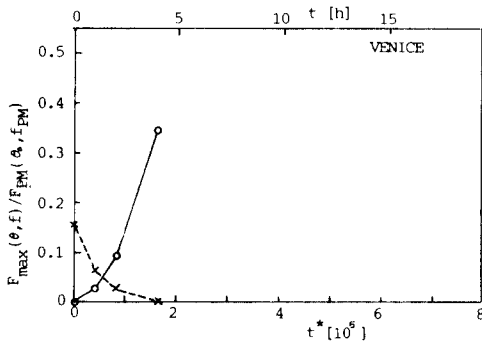


Fig. 7.2 Same as Fig. 7.1 for the DP model VENICE

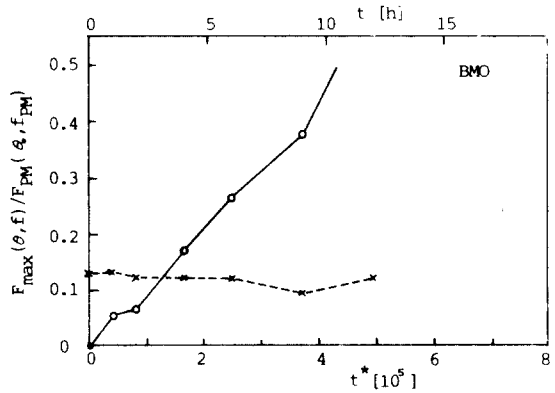


Fig. 7.3 Same as Fig. 7.1 for the CD model BMO

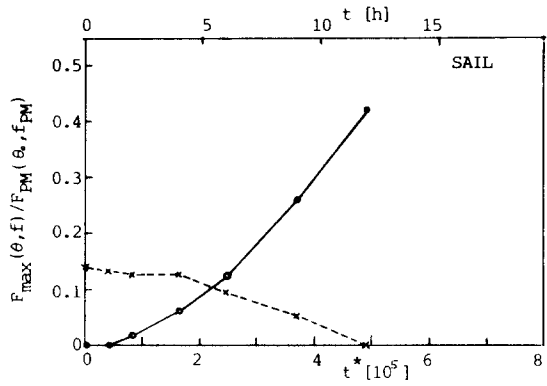


Fig. 7.4 Same as Fig. 7.1 for the CD model SAIL

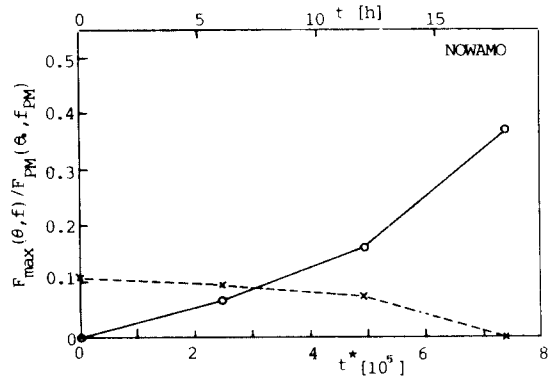


Fig. 7.5 Same as Fig. 7.1 for the CH model NOWAMO

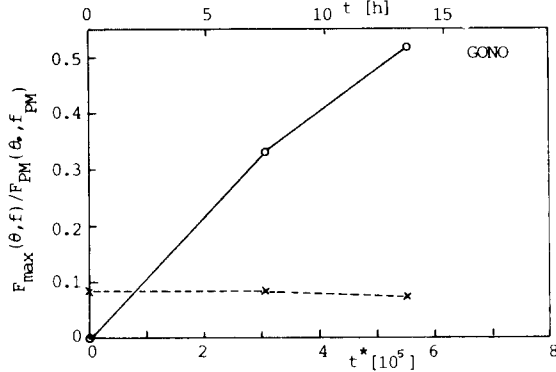


Fig. 7.6 Same as Fig. 7.1 for the model GONO

5. Conclusions

We see that:

- 1) The DP models show rapid fetch- and duration-limited growth rates.
- 2) The uncertainty in the drag coefficient relating to the friction velocity u^* to u_{10} should be investigated further.
- 3) The wide range of swell damping rates exist in the present models.
- 4) There should be a further study on the parameterization of the nonlinear transfer.
- 5) The extension of the proposed model to depth dependent model is needed to apply it to real time forecasting.

References

- 1) SWAMP Group, "Ocean Wave Modeling", Plenum Press, NY and London, 1985
- 2) SWIM Group, "Shallow Water Intercomparison of Wave Prediction Models(SWIM)", submitted for publication in Quart. J.R.Met. Soc., 1984
- 3) Neu, W.L. and S.H. Kwon, "A Directional Growth Mechanism for SOWM-type Wave Model", VPI-AOE-150, 1985
- 4) Kwon, S.H., "A Directional Growth of wind Generated Waves", PH. D. dissertation, Virginia Polytechnic Institute and State University, 1986
- 5) Neu, W.L. and S.H. Kwon, "A Directional Growth Mechanism for Numerical wave Model", 20th International Conference on Coastal Engineering in Taipei, Taiwan, 1986
- 6) Phillips, O.M., "On the Generation of Surface Waves by Turbulent Wind", J. Fluid Mech., 2, pp. 417-445, 1957
- 7) Miles, J.W., "On the Generation of Surface Waves by Shear Flow", part 1, J. Fluid Mech., 3, pp. 185-204, 1957
- 8) Miles, J.W., "On the Generation of Surface Waves by Shear Flow", part 2, *ibid.*, 6, pp. 568-582, 1959
- 9) Miles, J.W., "On the Generation of Surface Waves by Shear Flow", part 3, *ibid.*, 6, pp. 583-598, 1959
- 10) Miles, J.W., "On the Generation of Surface Waves by Shear Flow", part 4, *ibid.*, 7, pp. 469-478, 1960
- 11) Hasselmann, K., "Grungleichungen der Seegangsverossage", Schiffstechnik, 7, pp. 191, 1960
- 12) Barnett, T.P., "On the Generation, Dissipation, and Prediction of Ocean Wave", Geophys. Res., 73, 513-529, 1968
- 13) Ewing, J.A., "A Numerical Wave Prediction Method for the North Atlantic Ocean", Dtsch. Hydrogr. Z., 24, pp. 241-261, 1971
- 14) Gelci, R. and P. Chavy, "Seven Years of Numerical Wave Prediction with the DSAS Model in the Turbulent Fluxes through the Sea Surface", Wave Dynamics and Predictionn (A. Favre ad K. Hasselmann, eds.), Plenum Press, New York, pp. 565-591, 1978
- 15) Pierson, W.J., "The Spectral Ocean Wave Model (SOWM), A Northern Hemishers Computer Model for Specifying and Forecasting Ocean Wave Spectra", DTNSRDC-82/011, 1982
- 16) Hasselmann, K., al. et "A Parametrical wave Prediction Model", J. Phys. Oceanogr., 6, pp. 200-228, 1976
- 17) Gunter, H., W. Rosenthal and K. Richter, "Application of the Parametrical Surface Wave Prediction Model to Rapidly Varying Wind Fields during JONSWAP 1973", J. Geophys. Res., 84(18), pp. 4855-4864, 1979

- 18) Resio, D. T., "The Estimation of Wind-wave Generation in a Discrete Spectral Model", J. Geophys. Oceanogr., 11, pp. 510-525, 1981
- 19) Golding, B., "A wave Prediction System for Real-time Sea State Forecasting", Quart. J.R. Met. Soc., 109, pp. 393-416, 1983
- 20) Phillips, O. M., "The Dynamics of the Upper Ocean", Cambridge University Press, NY, 1966
- 21) Wu, J., "Laboratory Studies of Wind Wave Interactions", J. Fluid Mech., 34, part 1, pp. 91-111, 1969
- 22) Pierson, W. J. and Moskowitz, "A Proposed Spectral Form for Fully Developed Seas Based on the Similarity Theory of S. A. Kitagorodskii". J. Geophys. Res., 69, 5181-5203, 1964
- 23) Cote, L. J., et al., "The Directional Spectrum of a Wind Generated Sea as Determined from Data Obtained by the Stereo Wave Observation Project", Meteo. pap. vol. 2, No. 6, New York University, NY, pp. 88, 1960
- 24) Gadd, A. J., "A Numerical Advection Scheme with Small Phase Errors", Quart. J.R. Met. Soc., vol. 104, pp. 583-594, 1978
- 25) Gadd, A. J., "A Split Explicit Integration Scheme for Numerical Weather Prediction", ibid, vol. 104, pp. 569-582, 1978
- 26) Gadd, A. J., "Two Refinements of the Split Explicit Integration Scheme", ibid., vol. 106, pp. 215-220, 1980

◆

국제 학술대회 개최 안내

제23차 학회간 에너지 전환공학 학술대회

--23rd Intersociety Energy Conversion Engineering Conference--

주관: 미국기계학회(ASME)

후원: 미국기계학회를 포함한 7개 참여학회 및 3개 협동학회

분야: 대체연료, 바이오매스, 브레이튼 사이클, 열병합발전, 화석연료, 연료전지, 전기추진, 전기화학적에너지, 에너지절약, 에너지저장시스템, 지열동력, 수소에너지시스템, 원자핵 분열, 원자핵융합, 광전지, 랭킨사이클, 태양에너지전환, 태양열가열 및 냉각, 스팀링사이클, 열전기동력, 풍력등.

일시: 1988년 7월 31일~8월 5일

장소: 미국 Colorado주 Denver시 Denver Marriott Hotel